*Desalination and Water Treatment*
www.deswater.com

doi: 10.5004/dwt.2018.22123

109 (2018) 261–270
March

# Kinetic, isothermal, and thermodynamic models to evaluate Acid Blue 161 dye removal using industrial chitosan powder

Guilherme Dilarri*, Renato Nallin Montagnolli, Ederio Dino Bidoia, Carolina Rosai Mendes, Carlos Renato Corso

*Department of Biochemistry and Microbiology, São Paulo State University (UNESP), 24-A Avenue, 1515, Postal Code: 13506-900, Rio Claro-SP, Brazil, emails: dilarri@rc.unesp.br (G. Dilarri), renatonm@rc.unesp.br (R.N. Montagnolli), ederio@rc.unesp.br (E.D. Bidoia), carol.rosai.mendes@gmail.com (C.R. Mendes), crcorso@rc.unesp.br (C.R. Corso)*

Received 14 August 2017; Accepted 26 February 2018

**ABSTRACT**

Textile dyes are often discarded into the environment. Most of them are toxic and their release leads to severe impacts. This study evaluated the potential of industrial chitosan powder as an adsorbent material capable of removing such toxic compounds from aqueous solutions. Our experimental approach evaluated the removal of Acid Blue 161 azo textile dye. We further investigated the kinetics, isotherms, and thermodynamics of the chitosan-mediated adsorption. The chitosan powder had a high rate of dye adsorption, thus requiring only 111.45 mg of adsorbent to remove 100 μg $mL^{-1}$ of dye. It also reached equilibrium very rapidly (before 180 min), at a 20-min settling rate. We demonstrated that acidic pH increased the interaction between adsorbate/adsorbent, as the maximum adsorption capacity (10.301 μg $mL^{-1}$) occurred at pH 2.50. Kinetic studies indicated intraparticle diffusion of dye molecules in chitosan particles. The thermodynamic studies have shown that temperature influences the adsorption, in which higher temperatures improved adsorption. The thermodynamic analysis also showed that adsorption is an endothermic process. Fourier transform infrared spectroscopy confirmed that acidic pH triggered chemisorption and improved adsorbate/adsorbent interaction.

*Keywords:* Adsorption; Azo dyes; Chemisorption; Polymer; Textile dye; Waste

## 1. Introduction

Water pollution caused by industrial effluents is a worldwide issue due to the extensive environmental impacts on air, soil, and water quality. The textile industry is responsible for a large volume of contaminated wastewater containing dyes and other toxic organic compounds, such as benzene, toluene, ethylbenzene, naphthalene, anthracene, and xylene [1]. Up to 10% of these dyes are discharged during their production and consumption, thus representing a highly harmful pollution source to many ecosystems [2]. Most dyes exhibit high toxicity, including mutagenic and carcinogenic effects [3]. Dyes can also cause allergic dermatitis and skin sensitivity to animals, including humans. Such compounds may accumulate throughout the entire food chain and affect the global water cycle [2].

Azo dyes are the most commonly used textile dyes [4]. They are also the most discarded components found in textile effluents. Azo dyes are also considered to be the extremely toxic, due to the various aromatic molecules in their structure. The cleavage of their azo group (–N=N–) generates carcinogenic amine by-products that are much more toxic than the original structures [4].

There are several treatment techniques for dye-contaminated effluents, such as chemical and physicochemical processes, as well as biological degradation [5]. Adsorption is one of the most widely used techniques available for effluents contaminated with dyes. The main advantage of the

* Corresponding author.

adsorption methods is related to their low cost and biodegradability [6]. Another advantage is the rapid response in effluent treatment plants. Moreover, adsorption-based processes do not require large facilities. Many materials have already been described as good adsorbents, and most of them originate from waste or inexpensive by-products. Among these adsorbents, we can mention the coal coke, bentonite, resin, cotton, sand, rice hulls, palm tree straw, steel slag, feathers, steel waste, tannery waste, and the seed husks from *Araucaria* sp. [7]. However, the increasing need for large-scale adsorbent materials also involves the search for a universal material without regional restrictions. Most adsorbent materials are rendered infeasible because they are not widely available. This explains why activated carbon is still the leading adsorbent material for effluent treatment, even though its market value is much higher than other adsorbents [8]. In this context, it is imperative to propose new adsorbents that are capable of meeting industrial demand in large scale, along with minimal cost, and without supply and demand restrictions.

Chitosan, for example, is an adsorbent biopolymer that can be obtained by the deacetylation of chitin from the exoskeleton of arthropods and the cell walls of fungi. Chitosan has already been established as an adsorbent for the removal of textile dyes [9]. Several studies have reported modified forms of chitosan optimized for adsorption processes: chitosan flakes, microspheres, nanoparticles, biofilms, crosslinked chitosan, and chitosan with a high rate of deacetylation [10]. However, these changes end up increasing the price of this biopolymer. The high volume of textile dye contamination poses another challenge as the adsorbent material must keep up with industrial output. The total consumption of dyes in the world is estimated to be 10,000 ton/year [4].

Most of the industrially synthesized chitosan powder is from the food industry. Chitosan is derived from biowaste and can easily be synthesized from fishing residues, including shrimps, lobsters, and crayfish peels. These biomaterials are inexpensive in the global market. Moreover, chitosan can be harvested from fungal biomass as an inexhaustible and sustainable source of this biomaterial. In other words, the industrial chitosan powder is the ideal adsorbent due to its low cost and high availability that is not bound to any specific location.

There are many parameters that must be evaluated in the adsorption process: pH, temperature, and adsorbent mass. The sorption process may be influenced by the action of all those variables [8]. This study targets the current knowledge gap about chitosan-mediated adsorption kinetics and its thermodynamics. Our research provides a better understanding of the sorption process, narrowing down the possible adsorbate/adsorbent interactions with the textile dyes. The relevance of an in-depth study of chitosan lies in the total replacement of activated carbon that is currently applied to environmental cleanup processes.

Thus, the aim of this study was to evaluate the adsorptive potential of industrially synthesized chitosan powder for the removal of textile dyes. This is a novelty proposal since up to the present moment no work has ever studied industrial chitosan powder as an adsorbent material. Our research was carried out by varying the pH, temperature, and adsorbent mass to determine the best conditions for adsorption, therefore increasing its efficiency. Adsorption was also evaluated through kinetic models, isotherms, and thermodynamics. We investigated the ability of chitosan powder to remove dyes from aqueous solutions. The Acid Blue 161 dye was selected as the test subject to our adsorptive studies. Further analyses were conducted with Fourier transform infrared (FT-IR) spectrophotometer to evaluate both chitosan powder and dye molecules before and after the adsorption, seeking to unravel the main adsorbate/adsorbent interaction sites, as well as to confirm the occurrence of physisorption or chemisorption.

## 2. Materials and methods

### 2.1. Chitosan

Chitosan powder was obtained from Purifarma Chemistry & Pharmaceutical Ltda. – Brazil-SP. This chitosan was obtained from exoskeleton of crustaceans, 90% deacetylated, with $5.60 \times 10^{-3}$ mol of amino groups per gram of biopolymer, 80 mesh grain size, pH 7.50 and 0.38 g $mL^{-1}$ of density.

### 2.2. Dye

The azo dye used in this work was the Acid Blue 161 (AB 161), obtained from Sigma-Aldrich Chemical Company Inc (Taufkirchen, Germany). (Chemical Abstract Service (CAS) number 12392-64-8). It is soluble in water, pH 4.50, 40% purity and molecular weight 416.39 g $mol^{-1}$. A stock solution was prepared by dissolving 1 g of AB 161 in 1 L of deionized water. Our stock solution was stored in an amber glass flask in the dark at room temperature.

### 2.3. Bathochromic and hypsochromic shift

The bathochromic and hypsochromic shift showed if the dye changed its spectral band position. Dilutions of the stock solution (100 μg $mL^{-1}$) were prepared at different pH values (2.50, 4.50, 6.50, and 8.50). The solutions were analyzed in a UV–Vis spectrophotometer Model 2401 – PC (Shimadzu, Kyoto, Japan), within the 200–800 nm range in a 10 mm wide quartz cuvette.

After that, adsorption assays were performed using 20 mL of dye solutions at pH 4.50 in a 100 μg $mL^{-1}$ concentration at 293.15 ± 1 K, stirred at 150 rpm, at various chitosan powder masses (10, 20, 30, 40, 50, 60, 70, 80, and 90 mg). The adsorbate was in contact with the adsorbent for 3 h and then centrifuged at 3,000 rpm for 15 min to separate the chitosan powder from the supernatant. This setup allowed us to determine the mass of adsorbent required to adsorb all of the adsorbates.

### 2.4. Adsorption kinetics

Kinetic experiments were performed using 20 mL of 100 μg $mL^{-1}$ dye solution at pH 4.50 and 50 mg of chitosan powder. The dye solution was kept in contact with the adsorbent for 3 h at 293.15 ± 1 K and constant stirring (150 rpm). The sample was analyzed in a UV–Vis spectrophotometer every 30 min. The supernatant was centrifuged for 15 min at 3,000 rpm before each analysis. The amount of dye adsorption was calculated using Eq. (1):

$$q_e = \frac{V \cdot (C_o - C_e)}{W} \quad (1)$$

where $q_e$ is the equilibrium adsorbate concentration on the adsorbent (μg mg$^{-1}$), $V$ is the volume of adsorbate (mL), $C_o$ and $C_e$ are the initial and equilibrium concentration of adsorbate solution (μg mL$^{-1}$), respectively, and $W$ is the mass of adsorbent (mg).

### 2.5. Isotherm study

Various 100 μg mL$^{-1}$ dye-containing solutions ranging from pH 2.50 to 8.50 were prepared in 20 mL flasks. The mass of chitosan powder varied from 20 to 60 mg in this experimental step. The assays were conducted at a constant temperature (293.15 ± 1 K) and stirring (150 rpm).

The thermodynamic analysis was also conducted using 20 mL of 100 μg mL$^{-1}$ dye solutions. The temperature ranged from 283.15 to 323.15 K at pH 4.50, with constant stirring at 150 rpm. Chitosan powder mass was 50 mg.

In all of our isotherms assays, the adsorbate was in contact with the adsorbent up to final adsorption equilibrium time, which was previously determined in the kinetic studies. Each sample was centrifuged for 15 min at 3,000 rpm before each UV–Vis analysis.

All assays were performed in triplicate. Mathematical models were fitted to the dataset and verified according to their standard deviation (SD) values (Eq. (2)) [11]:

$$\mathrm{SD} = \sqrt{\frac{1}{N-1}\sum_{i=1}^{N}\left(\frac{Q_{ie} - Q_{ic}}{Q_{ie}}\right)^2} \quad (2)$$

where $Q_{ie}$ and $Q_{ic}$ are experimental and calculated mass of dye adsorbed by the adsorbent (μg mg$^{-1}$), respectively, and $N$ is the number of measurements.

### 2.6. Analysis by FT-IR spectrophotometry

Both chitosan powder and dye molecules were characterized by FT-IR spectrophotometer (Shimadzu Model 8300) before and after adsorption. The samples were heated at 378.15 K for 24 h in an incubator. Salt pellets were prepared using 149 mg of KBr and 1 mg of dry sample. Both were homogenized and compressed at 40 kN for 5 min. The pellets were placed in the FT-IR spectrophotometer sample holder as the absorbance was measured ranging from 400 to 4,000 cm$^{-1}$. Each of the 32 scans had a resolution of 4 cm$^{-1}$. Chemical structures were drawn using the ACD/ChemSketch software whereas the experimental data output was plotted using the Origin 6.10 software.

## 3. Results and discussion

### 3.1. Effect of bathochromic and hypsochromic shift

The AB 161 dye did not show bathochromic or hypsochromic shifts, therefore it has no isosbestic point. The dye was also stable to pH variations, which allowed us to perform all experimental assays at different pH ranges without concerns regarding chromophore band displacement.

We detected three chromophore groups: one at 563.55 nm, a smaller one at 373.92 nm and the maximum one at 603.82 nm. Thus, the UV–Vis spectrophotometer data were interpreted according to one of these chromophore groups. Certain reactive functional groups can absorb at different wavelengths in the visible spectrum, as they have more than one chromophore groups [12]. The most intense peak at 603.82 nm was subject to analysis as the main chromophore group.

Throughout the first adsorption study (Fig. 1), we determined the minimum amount of chitosan powder required to remove all the dye from the solution. A linear regression analysis provided the exact chitosan mass so that 20 mL of the dye solution (100 μg mL$^{-1}$) was removed by 111.45 ± 1 mg of chitosan powder at pH 4.50, 150 rpm, and 293.15 K,

The absorbance spectra of the dye did not change during the entire adsorption process. If absorbance had decreased without any changes in the spectrum, then all chemical structures related to the dye would have also been removed [13]. Chitosan powder was, in fact, effective towards an entire molecular absorption of the dye. The chemical group responsible for the dye toxicity was removed along with the adsorption process, yielding a reduced toxicological effect.

Another property of chitosan powder was related to its decantation. The separation of solid materials occurred in less than 20 min. This is a desirable feature in wastewater treatment plants. Despite the rapid decantation of chitosan powder, all samples were centrifuged before UV–Vis spectrophotometer analysis, to ensure that no particles of the adsorbent would disrupt the measurements.

### 3.2. Adsorption kinetics

According to the adsorption kinetics plot (Fig. 2), adsorption reached equilibrium in 180 min, with constant $q_e$. This effluent retention time is relevant to industrial waste treatment.

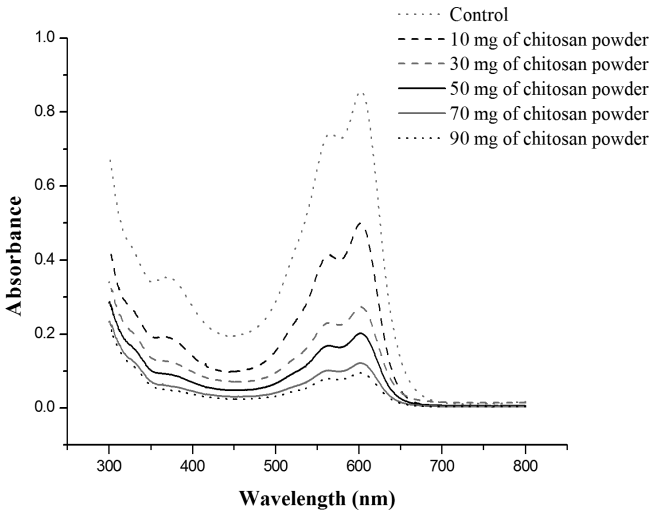


Fig. 1. Absorbance of AB 161 dye at pH 4.50 for different masses of chitosan powder.

The experimental $q_{e(exp)}$ was 1.667 μg mg$^{-1}$. However, an in-depth kinetic study further analyzed the process using pseudo-first and pseudo-second order kinetics. Thus, we could determine which of the two models were suitable to the process. We also examined the characteristics of adsorption, determining whether the rate-controlling process was based on mass transport (physical) or chemical interactions [14].

The pseudo-first order model was based on the adsorption capacity of solids [15]. The pseudo-first order model, as described by Lagergren [16], is shown in Eq. (3):

$$\ln\left(q_e - q_t\right) = \ln q_e - k_1.t \tag{3}$$

where $q_t$ is the amount of dye adsorbed (μg mg$^{-1}$), $t$ is time (min), and $k_1$ is the pseudo-first order adsorption rate constant (min$^{-1}$). A linear regression plot was made using $\ln(q_e - q_t)$ vs. $t$, to obtain $k_1$ and $q_{e(cal)}$.

In contrast to the pseudo-first order model, the pseudo-second order model was based on adsorption capacity, assuming that chemical adsorption controlled the process and adsorption was due to chemisorption [10]. The pseudo-second order model was developed by Ho and McKay [17] according to Eq. (4):

$$\frac{t}{q_t} = \frac{1}{k_s.q_e^{\,2}} + \frac{t}{q_e} \tag{4}$$

where $k_s$ is the pseudo-second order rate constant (mg μg$^{-1}$ min$^{-1}$), and in this case, $k_s$ and $q_{e(cal)}$ are calculated by linear regression ($t/q_t$) vs. $t$.

The kinetic analysis (Table 1) shows that the pseudo-second order kinetic model had the best fit to data, with a higher correlation coefficient than the pseudo-first order model. This result was supported by comparisons with experimental $q_{e(exp)}$ and calculated $q_{e(cal)}$ from our kinetic models. The $q_{e(cal)}$ from the pseudo-second order kinetic model was much closer to the $q_{e(exp)}$ values. In other words, adsorption was ruled by chemical interactions with electron exchanges between adsorbate and adsorbent [18].

Besides adsorption on the surface of the outer layer, the dye likely penetrated the chitosan powder, leading to biosorption. We used the intraparticle diffusion model proposed by Weber and Morris [19] (Eq. (5)) to confirm this phenomenon:

$$q_t = K_{\text{di}}.t^{0.5} + C \tag{5}$$

where $K_{\text{di}}$ is the constant intraparticle diffusion rate (mg μg$^{-1}$ [min$^{0.5}$]$^{-1}$) and $C$ is a constant related to the thickness of the diffusion layers (μg mg$^{-1}$).

When $q_t$ vs. $t^{0.5}$ is plotted, $K_{\text{di}}$ and $C$ values are determined according to intercept and slope values, as shown in Fig. 3.

According to Fig. 3, the two linear regions represent the boundary layer and the intraparticle diffusion inside the macropore [17]. The first linear region corresponds to surface adsorption during the initial contact between adsorbate and adsorbent. The second linear region corresponds to macropore diffusion and the occurrence of biosorption in chitosan powder [17]. Chitosan powder reached its equilibrium as the dye moved into the macropores at the final step of biosorption diffusion.

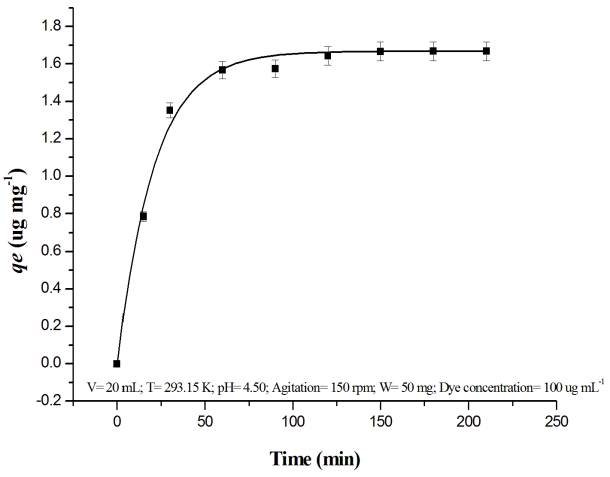


Fig. 2. Experimental adsorption kinetics.

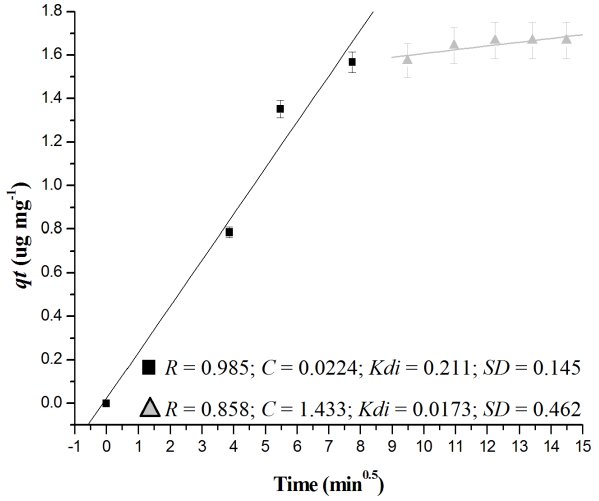


Fig. 3. Intraparticle diffusion.

Table 1
Kinetic model parameters

| Initial dye concentration (μg mL$^{-1}$) | $q_{e(exp)}$ (μg mg$^{-1}$) | Pseudo-first order | | | | Pseudo-second order | | | |
|---|---|---|---|---|---|---|---|---|---|
| | | $k_1$ (min$^{-1}$) | $q_{e(cal)}$ (μg mg$^{-1}$) | SD | $R$ | $k_s$ (mg μg$^{-1}$ min$^{-1}$) | $q_{e(cal)}$ (μg mg$^{-1}$) | SD | $R$ |
| 100.00 | 1.667 | 0.0130 | 0.677 | 0.437 | 0.922 | 0.0695 | 1.741 | 0.289 | 0.998 |

The low $K_{di}$ value of the macropore step indicates that intraparticle diffusion was fast at the first layer. The boundary layer did not act as a barrier to dye penetration. This is supported by the *C* value of the first boundary layer, where the layer thickness was much lower compared with the second layer of the macropore. Therefore, chitosan powder allows the diffusion of the AB 161 dye.

We used Eq. (6) developed by Boyd et al. [20] to determine whether the biosorption process occurs first by filling the adsorptive sites of the surface and then the diffusion, or if intraparticle diffusion occurs first by filling all the internal adsorptive sites and then the dye is adsorbed on the surface.

$$B_t = -0.4977 - \ln(1 - F) \tag{6}$$

and

$$F = \frac{q_t}{q_e} \tag{7}$$

where *F* is the fraction of solute adsorbed at any time *t*, and $B_t$ is the mathematical function of *F*.

If the $B_t$ vs. *t* plot passes through the origin, biosorption is controlled by intraparticle diffusion. Otherwise, if the line does not cross the origin of coordinates, biosorption is controlled by surface diffusion [21]. The $B_t$ vs. *t* plot (Fig. 4) showed that biosorption is ruled by surface diffusion. Thus, the main adsorption sites were on the surface of the adsorbent, indicating that intraparticle diffusion was not controlling the sorption process.

Using Eq. (7) by Boyd et al. [20], we calculated the effective diffusion coefficient ($D_i$). According to Singh et al. [22], if $D_i$ values do not remain on the order of $10^{-11}$ cm$^2$ s$^{-1}$, the intraparticle diffusion occurs after chitosan powder is completely filled at its external binding sites. The external sites are the actual sorption controllers when the energy of interaction with the adsorbate is high.

$$D_i = \frac{r^2.B_b}{\pi^2} \tag{8}$$

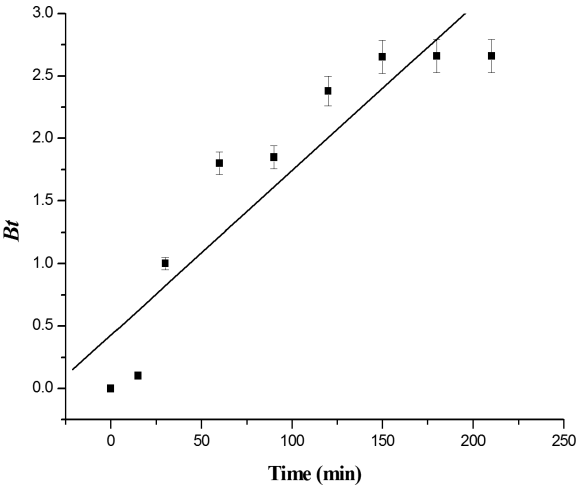


Fig. 4. Boyd function plot.

$B_b$ is calculated from $B_t$ as a function of *t*, where *r* is the average radius of the chitosan powder particle (0.0177 cm) and $D_i$ is the effective diffusion coefficient (cm$^2$ s$^{-1}$) of AB 161 dye in the chitosan powder.

The $D_i$ values were $1.043 \times 10^{-7}$ cm$^2$ s$^{-1}$, thus confirming that sorption is controlled by the external sites and that diffusion is proportional to the saturation of these sites.

### 3.3. Isotherm study

The isotherms determined the sorption and desorption equilibrium of solid/solution interfaces. The sorption mechanism (chemical or physical), the sorption and interaction sites, and the adsorbent/adsorbate affinity were also determined using isotherms [21]. In our work, we used the Langmuir and Freundlich isotherms.

The Langmuir model assumes that the adsorbent surface has a finite number of active sorption sites occupied by a single chemical structure of monolayers [23]. The Langmuir model suggests that interaction forces between adsorbed molecules are negligible [23]. Eq. (8) shows the mathematical model proposed by Langmuir [24] as follows:

$$\frac{C_e}{q_e} = \frac{1}{l.q_m} + \frac{C_e}{q_m} \tag{9}$$

where $q_m$ is the maximum quantity of adsorbate which adsorbed to the monolayer (μg mg$^{-1}$), and *l* is the Langmuir constant related to the affinity of adsorbent and adsorbate (mL mg$^{-1}$). The equilibrium parameters are the angular coefficient ($C_e/q$) vs. $C_e$.

The separation factor of the Langmuir constant was calculated using Eq. (9), proposed by McKay et al. [25] as follows:

$$R_l = \frac{1}{1 + l.C_0} \tag{10}$$

where $R_l$ is the separation factor in the Langmuir model. From the value of $R_l$, we determined whether adsorption is favorable or unfavorable: $R_l = 1$ the adsorption is linear, $R_l = 0$ the adsorption is an irreversible process, $R_l > 1$ the adsorption is unfavorable, $0 < R_l < 1$ the adsorption is favorable [25].

The second analysis was proposed by Freundlich [26]. This model was based on the sorption process of heterogeneous surfaces, where active sites are exponentially occupied and multiple layers are formed. The most energetic sites occupied first. Therefore, the intensity of site interactions decreased when sorption sites were filled with adsorbate [27]. The Freundlich model is shown in Eq. (10):

$$\ln q_e = \ln K_f + \frac{1}{n_f}.\ln C_e \tag{11}$$

where $K_f$ is the Freundlich constant of solid adsorption capacity (mL mg$^{-1}$), and $n_f$ is the adsorption intensity constant.

The adsorption process followed the Freundlich model in all of our assays (Table 2), even after variations in the pH

Table 2
Isotherms in variable pH of dye solution

| pH | Initial dye concentration (μg mL$^{-1}$) | $R_l$ | Langmuir isotherm | | | | Freundlich isotherm | | | |
|---|---|---|---|---|---|---|---|---|---|---|
| | | | $q_m$ | $l$ | SD | $R$ | $K_f$ | $n_f$ | SD | $R$ |
| | 100.00 | | | | | | | | | |
| 2.50 | | 0.395 | 10.301 | 0.0139 | 0.380 | 0.800 | 0.187 | 1.022 | 0.282 | 0.996 |
| 4.50 | | 0.206 | 3.525 | 0.0350 | 0.534 | 0.955 | 0.219 | 1.589 | 0.462 | 0.978 |
| 6.50 | | 0.378 | 1.909 | 0.0150 | 1.074 | 0.950 | 0.00091 | 0.457 | 0.896 | 0.974 |
| 8.50 | | 0.412 | 0.806 | 0.0130 | 3.398 | 0.917 | 0.00001 | 0.330 | 1.139 | 0.957 |

of the dye solution. We also observed that $q_m$ (calculated using the Langmuir model) decreased as the pH of the solution increased. The $R_l$ parameter from the Langmuir model corroborates this result. Despite having an $R_l < 1$ (meaning favorable adsorption), the $R_l$ value also increased proportionally to the pH rise, thus indicating an unfavorable adsorption at high pH. The pH 8.50 had the highest $R_l$ value and the least efficient adsorption, with the lowest interaction between adsorbate/adsorbent compared with other pH values.

The $K_f$ values indicated that adsorbent capacity decreased as the pH increased. The values of $n_f$ at pH 2.50 and 4.50 were higher than 1, meaning that adsorption was favorable. Wong et al. [28] had reported a similar adsorption pattern. Any $n_f$ values above 1 would indicate side chemical interactions among different adsorbates and the formation of multiple layers [29]. However, the $n_f$ values ranging from 0.9 to 1.1 found in our acidic pH conditions, pointed towards chemisorption [28]. This dataset confirmed our previous assumptions about the chemical interactions according to the pseudo-second order kinetics.

The assays with pH 6.50 and 8.50 resulted in $n_f < 1$, which is related to unfavorable adsorption and processes that are not controlled by chemisorption [28]. Moreover, the $n_f < 1$ indicated that no lateral interactions between the adsorbate occurred [29]. Neither chemical interaction nor diffusion occurred as well. Physical adsorption was likely due to near neutral pH and van der Waals forces.

The $q_m$ parameter allowed us to compare the maximum sorption capacity of industrial chitosan powder with other adsorbent materials containing chitosan. Most studies applied synthesis and complexation of the biopolymer with others agents in order to increase the adsorptive capacity of chitosan [30–32]. Ngah et al. [30], for example, used crosslinked chitosan-coated bentonite to remove the tartrazine dye, as it increased the removal efficiency of the biopolymer by reaching at a minimum $q_m$ value of 250.0 mg g$^{-1}$.

Another example of modification was investigated by Dilarri and Corso [31], as they complexed chitosan in spheres and immobilized microorganisms inside of these materials. They analyzed three different chitosan-derived adsorbents to reach minimum values of $q_m$ (27.661, 31.037, and 55.401 μg mg$^{-1}$). Despite these high values of $q_m$, the changes in chitosan also increased the cost of the adsorbent, leading to steep rise in the treatment price. Besides, the chemical modifications of the biopolymer are not feasible on an industrial scale, thus limiting the demand for such adsorbent usage in a textile effluent treatment plant.

The maximum quantity of adsorption capacity in our study was higher than reported by Tanhaei et al. [32]. It should be taken into account that adsorbate changes can also change the values of $q_m$, due to new adsorbate/adsorbent interactions [31], thus rendering direct comparisons with other adsorption studies a very challenging task.

Still, Annadurai et al. [29] studied chitosan without going through chemical complexing processes. Their results showed that minimum $q_m$ reached of 91.47 mg g$^{-1}$ in the removal of Remazol Black 13 dye. There is indeed a substantial difference in $q_m$ values found between this and their study. However, it must be taken into account that their tests were performed at different concentrations, temperature, and pH. Still, the studies performed by Annadurai et al. [29] corroborate with our data, indicating that chitosan is a good adsorbent material even without undergoing any chemical modification. This further emphasizes the need to study industrially produced chitosan as an adsorbent agent.

The thermodynamic analysis determined if the adsorption process was spontaneous, exothermic, or endothermic [29]. The advantage of our thermodynamic approach was that we were able to confirm if temperature heavily influenced adsorption. Eq. (11) by Van't Hoff was used to calculate the thermodynamic parameters:

$$\ln K_d = \frac{\Delta s}{R} - \frac{\Delta H}{R}.\frac{1}{T} \tag{12}$$

and

$$K_d = \frac{q_e}{C_e} \tag{13}$$

where $K_d$ is the equilibrium constant from temperature variations (mol g$^{-1}$), $T$ is the temperature (K), and $R$ is the universal gas constant (8.314 J mol$^{-1}$ K$^{-1}$). $\Delta S$ is entropy and $\Delta H$ is the sorption enthalpy.

A $\ln K_d$ vs. ($1/T$) plot was analyzed, as the slope and intercept allowed the calculation of entropy and enthalpy values. The Gibbs free energy ($\Delta G$) was given by Eq. (12):

$$\Delta G = \Delta H - (\Delta S.T) \tag{14}$$

According to thermodynamic analysis (Table 3), $\Delta H$ is positive, thus indicating an endothermic process. The positive entropy value relates to chemical bond randomness at

Table 3
Thermodynamic analysis

| Initial dye concentration (μg mL$^{-1}$) | SD | $\Delta S$ (kJ mol$^{-1}$ K$^{-1}$) | $\Delta H$ (kJ mol$^{-1}$) | $\Delta G$ (kJ mol$^{-1}$) | | | |
|---|---|---|---|---|---|---|---|
| | | | | 283.15 K | 293.15 K | 303.15 K | 323.15 K |
| 100.00 | 0.540 | 0.0015 | 7.461 | 7.036 | 7.021 | 7.006 | 6.976 |

solid–solution interfaces. In other words, there was more than one adsorption-binding site. This result is further expanded by our Freundlich isotherms, in which the binding sites were heterogeneous and had more than one linkage mechanism with the AB 161 dye.

The Gibbs free energy continuously decreased as the temperature increased, confirming that the sorption is influenced by temperature. The higher the temperature, the more interactions between adsorbate/adsorbent occurs, thus favoring adsorption. Despite the positive values of Gibbs free energy, it is possible to affirm that the adsorption is a spontaneous process since its values are decreasing as the temperature increases. Therefore, a natural interaction between adsorbate/adsorbent was observed [33]. Nevertheless, isotherms and thermodynamic studies showed a reasonable variation of several parameters, among them the pH and temperature. Even though Gibbs free energy had positive values (endothermic adsorption) our kinetic and isothermal results pointed towards a strong interaction between adsorbate/adsorbent [33]. The adsorption occurred in all of them within the specified experimental range, leading to a spontaneous adsorption. In spite of this result, the dyes had 40% purity. The other 60% of its composition was mostly ionic salts such as NaCl, $MgCl_2$ among others. Those dissolved salts were not enough to compete or to disfavor the adsorption of the dye AB 161 by the chitosan powder.

### 3.4. FT-IR spectrophotometry analysis

Fig. 5 shows the characterization of AB 161 by FT-IR spectrophotometer before the adsorption assays. We observed intense bands in 1,566; 1,369; 1,139; and 667 cm$^{-1}$ region, corresponding to the chemical azo group –N=N–; the –C–H; –C=C– bonds, and =C–C in aromatic rings. The peak in 1,458 cm$^{-1}$ represented the stretching of the –C–N bonds, as the region was possibly related to the azo group. The peak in 758 cm$^{-1}$ corresponded to the deformation of –C–H bonds in aromatic rings. The peak in 1,049 cm$^{-1}$ corresponded to the sulfonic group vibration.

The bands within the 2,843–2,924 range and 3,433 cm$^{-1}$ are $CO_2$ residues from the air and residual primary amines present in the sample, respectively. The peaks were all consistent with the AB 161 dye structure (Fig. 6).

A similar FT-IR spectrum from chitosan powder before any adsorption study (Fig. 7) was also found by Ko et al. [34]. Their absorption bands occurred at 2,927; 1,659; 1,377; 1,070; and 623 cm$^{-1}$; identified as –OH, –NH, –$NH_2$, –C–O, and –C–OOH bonds, respectively. The 1,312 cm$^{-1}$ peak indicated vibrations at carbon bonds in cyclic groups. The bands in the 2,358 and 3,421 cm$^{-1}$ regions indicated residues of atmospheric carbon and primary amine.

The chitosan spectrogram is consistent with the chemical structure of chitosan in Fig. 8.

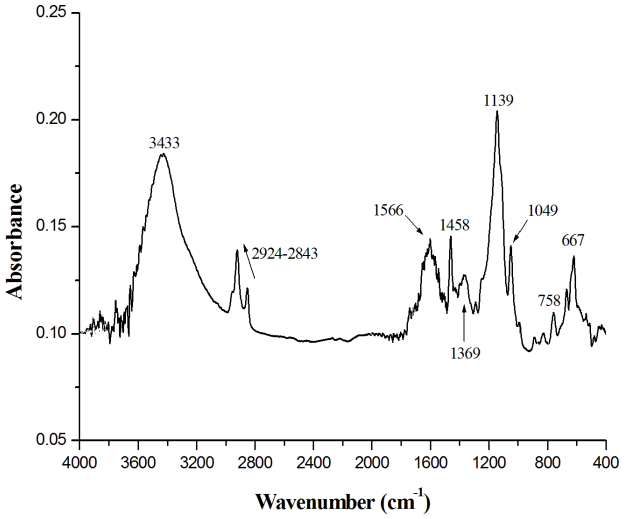


Fig. 5. Characterization of dye AB 161 by FT-IR spectrophotometer.

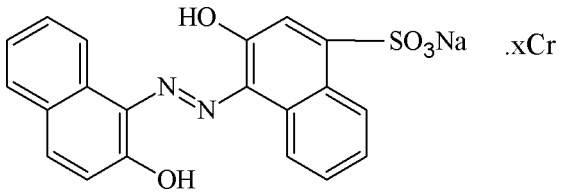


Fig. 6. Chemical structure of Acid Blue 161 dye.

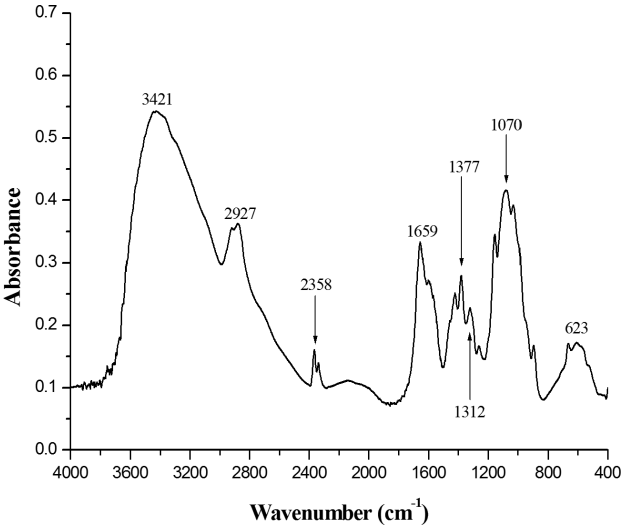


Fig. 7. Characterization of industrial chitosan powder by FT-IR spectrophotometer.

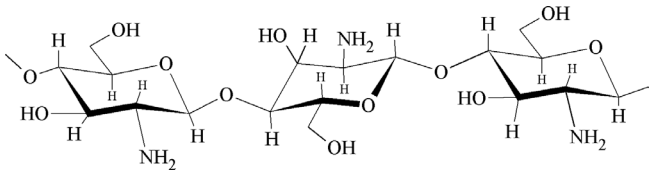

Fig. 8. Chemical structure of chitosan.

The FT-IR was a useful tool to identify possible adsorption links. We confirmed whether the adsorption was a chemical or a physical process [35] based on the variations of FT-IR spectra before and after the sorption process. Any changes in the spectrum would indicate the occurrence of a new chemical bond that did not initially exist [9], that is, chemisorption. On the other hand, an immutable FT-IR spectrum after adsorption would indicate physisorption [9]. Thus, FT-IR spectra before adsorption not only characterized the adsorbate/adsorbent but also acted as a primary reference on what kind of interaction was taking place during adsorption.

The FT-IR spectrum of chitosan powder after adsorption (Fig. 9) at acidic conditions outputted more intense bands. The peaks at 1,659; 1,377; and 1,598 $cm^{-1}$ represented –NH, $–NH_2$, and $–NH_3^+$ binding of chitosan, respectively. The protonated binding site in chitosan at low pH is a dye attachment site.

The peaks at 1,419 and 1,319 $cm^{-1}$ were vibrations of azo groups and –C–H bonds of aromatic rings. The vibrations were enhanced due to the dye molecule [35]. A small difference in the 1,258 $cm^{-1}$ peak is related to the vibration of amine bonds between dye and chitosan [9]. The 1,153 $cm^{-1}$ peak corresponds to sulphonic groups $SO_3^-$, where the $SO_3^-$ dye group would be a possible chitosan-binding region. The peaks in 1,076 and 1,049 $cm^{-1}$ corresponded to the linking groups –C–C and –C–O from the aromatic rings of the dye. The peaks in 664 and 623 $cm^{-1}$ were due to –H–C and –C–OOH bonds, respectively.

The acidic pH requires amino functional groups ($NH_2$) of chitosan to be protonated ($NH_3^+$) groups (Fig. 10). The AB 161 dye dissolved in water and had a sulfonic group ($SO_3^-$), leading to a more efficient interaction between adsorbent and adsorbate. Ionic interactions occurred (Fig. 10), as evidenced by our kinetic, isotherm, and thermodynamic studies. The FT-IR spectrum of the chitosan powder after adsorption at an acid pH corroborated our initial hypothesis: we detected a high intensity of bands combined with structural modifications of the spectrum in the respective regions, thus confirming the occurrence of chemisorption. The more acidic the pH, the higher the formation of hydrogen bonds. The –H bonds promoted bond formation between the dye and chitosan, as shown in Fig. 10.

Chitosan powder after adsorption in alkaline pH showed no enhancements according to their FT-IR band profile, thus confirming the physical interaction between dye and chitosan. Such physisorption at alkaline pH matched our isothermal studies. Moreover, the results explained the lower adsorptive intensity at pH 6.50 and 8.50, as physisorption is weaker than chemisorption. The adsorption at both alkaline pH was due to physical van der Waals interactions.

The FT-IR spectrophotometry confirmed the strong chemical interaction between dye and chitosan powder.

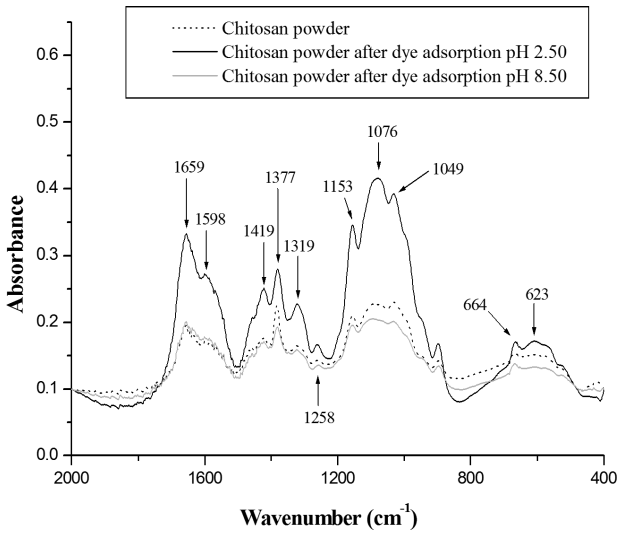


Fig. 9. FT-IR spectrum of chitosan powder before and after adsorption of AB 161 dye in acid and alkaline pH.

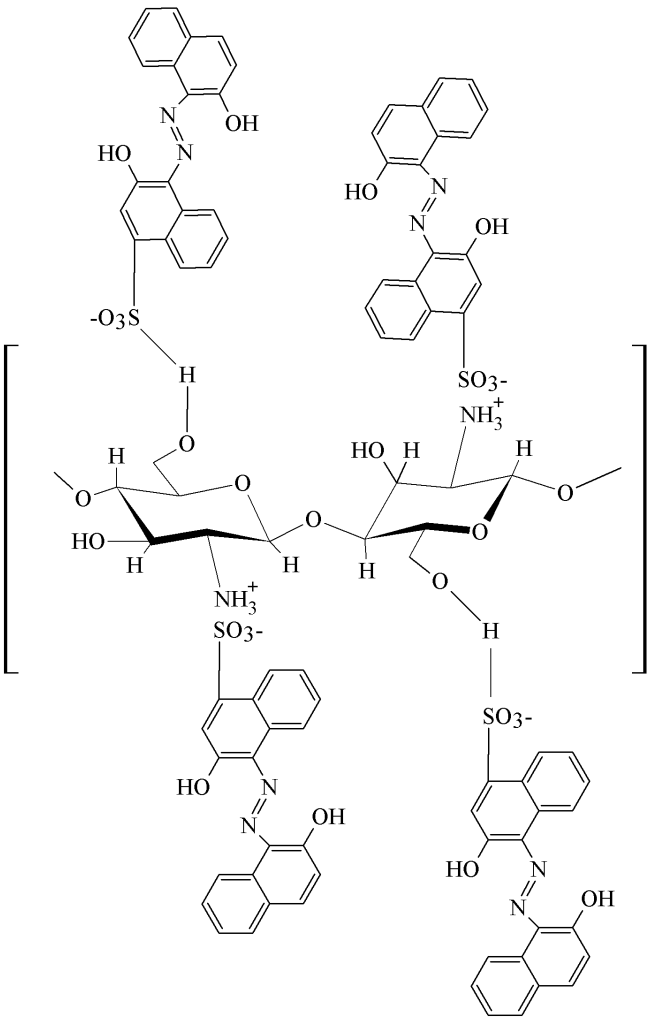

Fig. 10. Proposed structure of the chemical bond between the AB 161 dye and chitosan powder in acid pH.

It is safe to assume that separation is difficult, even though desorption was not determined. Desorption is an important process because it allows the reuse of the adsorbent materials, thus reducing the treatment costs [36]. The process, however, can be prohibitively expensive depending on desorption efficiency. Chitosan originates from biowaste, with its low production associated with synthesis at an industrial scale. In this case, desorption may not be the most cost-effective alternative, as it is not necessary. Our kinetic studies showed that chitosan powder reached its maximum equilibrium point when binding all of its adsorptive sites with the adsorbate. The process results in complete adsorbent saturation without removing any more molecules of dye from the solution. Therefore, reuse of chitosan powder is unfeasible after equilibrium state is reached.

## 4. Conclusion

Chitosan powder reached its adsorption equilibrium in 180 min. Such fast equilibrium response is an important characteristic of biosorbents, along with intraparticle diffusion that further enhances the adsorption area. The isotherms determined the maximum adsorption capacity at 10.301 μg $mg^{-1}$ in pH 2.50, as well as the types of bonds between the dye and chitosan powder. The most effective chemical interaction occurred at acidic pH, thus proving that the higher the pH the lower the sorption. According to our thermodynamic analyses, adsorption was an endothermic process, and its efficiency increases with temperature. We propose that chemisorption in acidic pH is due to the protonation of chitosan binding sites and hydrogen bonding. On the other hand, alkaline pH may cause physisorption, which explains the low adsorption intensity of chitosan. The pH directly influenced the adsorption of chitosan powder.

Whereas pH has a considerable influence over chitosan activity, the AB 161 dye itself was stable to pH variations. There was no displacement of its visible spectrum. Still, industrial chitosan powder gave a reasonable and effective adsorption capacity in our experimental conditions. We achieved the removal of up to 100 μg $mL^{-1}$ of AB 161 using a very small chitosan amount (111.45 ± 1 mg). The industrial chitosan powder decanted rapidly, which is a desirable feature of adsorbent materials. Therefore, we argue that there is a high potential for the industrial treatment of textile effluents using chitosan powder. Especially because the worldwide abundance of chitosan as a waste material from fishing-related activities could easily meet industrial demand in large-scale treatment plants.

## Acknowledgement

Support from the Brazilian fostering agencies: Conselho Nacional de Desenvolvimento Científico e Tecnológico (CNPq) – Brazil.

## References

[1] R. Gong, X. Zhang, H. Liu, Y. Sun, B. Liu, Uptake of cationic dyes from aqueous solution by biosorption onto granular kohlrabi, Bioresour. Technol., 98 (2007) 1319–1323.
[2] H.S. Ghazi Mokri, N. Modirshahla, M.A. Behnajady, B. Vahid, Adsorption of C.I. Acid Red 97 dye from aqueous solution onto walnut shell: kinetics, thermodynamics parameters, isotherms, Int. J. Environ. Sci. Technol., 12 (2015) 1401–1408.
[3] O. Yesilada, D. Asma, S. Cing, Decolorization of textile dyes by fungal pellets, Process Biochem., 38 (2003) 933–938.
[4] N.P. Raval, P.U. Shah, N.K. Shah, Adsorptive amputation of hazardous azo dye Congo red from wastewater: a critical review, Environ. Sci. Pollut. Res., 23 (2016) 14810–14853.
[5] H.S. Rai, M.S. Bhattacharyya, J. Singh, T.K. Bansal, P. Vats, U.C. Banerjee, Removal of dyes from the effluent of textile and dyestuff manufacturing industry: a review of emerging techniques with reference to biological treatment, Crit. Rev. Environ. Sci. Technol., 35 (2005) 219–238.
[6] A.N. Módenes, F.R. Espinoza-Quiñones, C.A.Q. Geraldi, D.R. Manenti, D.E.G. Trigueros, A.P. Oliveira, C.E. Borba, A.D. Kroumov, Assessment of the banana pseudostem as a low-cost biosorbent for the removal of reactive blue 5G dye, Environ. Technol., 36 (2015) 2892–2902.
[7] H. Wang, Y. Wang, H. Yan, Binding of sodium dodecyl sulfate with linear and branched polyethyleneimines in a aqueous solution at different pH values, Langmuir, 22 (2006) 1526–1533.
[8] P. Sharma, H. Kaur, M. Sharma, V. Sahore, A review on applicability of naturally available adsorbents for the removal of hazardous dyes from aqueous waste, Environ. Monit. Assess., 183 (2011) 151–195.
[9] W.S.W. Ngah, A. Kamari, S. Fatinathan, P.W. Ng, Adsorption of chromium from aqueous solution using chitosan beads, Adsorption, 12 (2006) 249–257.
[10] G. Crini, P.M. Badot, Application of chitosan, a natural aminopolysaccharide, for dye removal from aqueous solution by adsorption process using batch studies: a review of recent literature, Prog. Polym. Sci., 33 (2008) 399–447.
[11] H. Mazaheri, M. Ghaedi, A. Asfaram, S. Hajati, Performance of CuS nanoparticle loaded on activated carbon in the adsorption of methylene blue and bromophenol blue dyes in binary aqueous solutions: using ultrasound power and optimization by central composite design, J. Mol. Liq., 219 (2016) 667–676.
[12] E.K. Mitter, C.R. Corso, Acid dye biodegradation using *Saccharomyces cerevisiae* immobilized with polyethyleneimine-treated sugarcane bagasse, Water Air Soil Pollut., 224 (2013) 1391–1398.
[13] J.K. Glenn, M.H. Gold, Decolorization of several polymeric dyes by the lignin-degrading Basidiomycete *Phanerochaete chrysosporium*, Appl. Environ. Microbiol., 45 (1983) 1741–1747.
[14] Y. Safa, H.N. Bhatti, M. Sultan, S. Sadaf, Synthesis, characterization and application of wheat bran/zinc aluminium and tea leaves waste/zinc aluminium biocomposites: kinetics and thermodynamics modeling, Desal. Wat. Treat., 57 (2016) 25532–25541.
[15] M. Hasan, A.L. Ahmad, B.H. Hameed, Adsorption of reactive dye onto cross-linked chitosan/oil palm ash composite beads, Chem. Eng. J., 136 (2008) 164–172.
[16] S. Lagergren, Zurtheorie der sogenannten adsorption gel osterstoffe, K. Sven. Vetensk.akad. Handl., 24 (1898) 1–39.
[17] Y.S. Ho, G. McKay, Sorption of dye from aqueous solution by peat, Chem. Eng. J., 70 (1998) 115–124.
[18] B.K. Nandi, A. Goswami, M.K. Purkait, Adsorption characteristics of brilliant green dye on kaolin, J. Hazard. Mater., 161 (2009) 387–395.
[19] W.J. Weber, J.C. Morris, Kinetics of adsorption on carbon from solution, J. Sanit. Eng. Div. Am. Soc. Civil Eng., 89 (1963) 31–60.
[20] G.E. Boyd, A.W. Adamson, L.S. Myers, The exchange adsorption of ions from aqueous solution by organic zeolites, II. Kinetics, J. Am. Chem. Soc., 69 (1947) 2836–2848.
[21] R. Aravindhan, J.R. Rao, B.U. Nair, Removal of basic yellow dye from aqueous solution by sorption on green algae *Caulerpa scalpelliformis*, J. Hazard. Mater., 142 (2007) 68–76.
[22] K.P. Singh, D. Mohan, S. Sinha, G.S. Tondon, D. Gosh, Color removal from wastewater using low-cost activated carbon derived from agricultural waste material, Ind. Eng. Chem. Res., 42 (2003) 1965–1976.
[23] P. Podkoscielny, K. Nieszporek, Adsorption of phenols from aqueous solutions: equilibria, calorimetry and kinetics of adsorption, J. Colloid Interface Sci., 354 (2011) 282–291.

[24] I. Langmuir, The adsorption of gases on plane surface of glass, mica and platinum, J. Am. Chem. Soc., 40 (1918) 1361–1368.
[25] G. McKay, H.S. Blair, J.R. Gardner, Adsorption of dyes on chitin: equilibrium studies, J. Appl. Polym. Sci., 27 (1982) 3043–3043.
[26] H. Freundlich, Adsorption in solution, Phys. Chem. Soc., 40 (1906) 1361–1368.
[27] R.I. Yousef, B. El-Eswed, A.H. Al-Muhtaseb, Adsorption characteristics of natural zeolites as solid adsorbents for phenol removal from aqueous solutions: kinetics, mechanisms and thermodynamics studies, Chem. Eng. J., 171 (2011) 1143–1149.
[28] Y.C. Wong, Y.S. Szeto, W.H. Cheung, G. McKay, Adsorption of acid dyes on chitosan equilibrium isotherms analysis, Process Biochem., 39 (2004) 693–702.
[29] G. Annadurai, L.Y. Ling, J.F. Lee, adsorption of reactive dye from an aqueous solution by chitosan: isotherm, kinetic and thermodynamic analysis, J. Hazard. Mater., 152 (2008) 337–346.
[30] W.S.W. Ngah, N.F.M. Ariff, M.A.K.M. Hanafiah, Preparation, characterization, and environmental application of crosslinked chitosan-coated bentonite for tartrazine adsorption from aqueous solutions, Water Air Soil Pollut., 206 (2010) 225.
[31] G. Dilarri, C.R. Corso, *Saccharomyces cerevisiae* immobilized onto cross-linked chitosan beads: application of a novel material for the removal of dye toxicity, Environ. Technol., (2017) http://dx.doi.org/10.1080/09593330.2017.1340351.
[32] B. Tanhaei, A. Ayati, M. Lahtinen, B.M. Vaziri, M. Sillanpaa, A magnetic mesoporous chitosan based core-shells biopolymer for anionic dye adsorption: kinetic and isothermal study and application of ANN, J. Appl. Polym. Sci., 133 (2016) 43466.
[33] J.Y. Farah, N.S. El-Gendy, Performance, kinetics and equilibrium in biosorption of anionic dye Acid Red 14 by the waste biomass of *Saccharomyces cerevisiae* as a low-cost biosorbent, Turk. J. Eng. Environ. Sci., 37 (2013) 146–161.
[34] Y.G. Ko, H.J. Lee, S.S. Shin, U.S. Choi, Dipolar-molecule complexed chitosan carboxylate, phosphate and sulphate dispersed electrorheological suspensions, Soft Matter, 23 (2012) 6273–6279.
[35] P. Monash, G. Pugazhenti, Adsorption of crystal violet dye from aqueous solution using mesoporous materials synthesized at room temperature, Adsorption, 15 (2009) 390–405.
[36] S. Sadaf, H.N. Bhatti, M. Arif, M. Amin, F. Nazar, Adsorptive removal of direct dyes by PEI-treated peanut husk biomass: Box–Behnken experimental design, Chem. Ecol., 31 (2015) 252–264.